

## Simulation of Effect of Various Distances between Front and Rear Body on Drag of a Non-Circular Cylinder

Open  
Access

Muhammad Fahmi Mohd Sajali<sup>1</sup>, Syed Ashfaq<sup>2</sup>, Abdul Aabid<sup>1,\*</sup>, Sher Afghan Khan<sup>1</sup>

<sup>1</sup> Department of Mechanical Engineering, Faculty of Engineering, International Islamic University Malaysia, Kuala Lumpur, Malaysia

<sup>2</sup> Department of Automobile Engineering, M.H. Saboo Siddik College of Engineering, Byculla, Mumbai, Maharashtra, India

### ARTICLE INFO

### ABSTRACT

#### Article history:

Received 24 June 2019

Received in revised form 21 August 2019

Accepted 2 October 2019

Available online 13 October 2019

Numerical investigation of a non-circular cylinder (D-shaped bluff body) of fore body, geometrical effects on the drag as well as on the flow-field were simulated at the subcritical flow regime at a velocity of 26.84 m/s. The non-circular cylinder (D-shaped model) front surface for a positive pressure of the unsteady vortex generation in the near wake, the square plate was attached upstream of the non-circular cylinder as the base model. The forebody modifies the streamlines that separate from its edges to attach smoothly onto the front face shoulders of the main body, thereby converting the bluff body into an equivalent streamlined body, resulting in minimum drag. The height of the forebody ( $B_1$ ) is 25 mm, and the length of the front body ( $L_2$ ), was in the range from  $0.25B_2$  to  $1.75B_2$ . The results obtained from the simulation are compared with the experimental results. The results indicate that the side faces and the rear faces are subjected to low pressure, whereas the front face is experiencing high positive pressure. With this flow pattern, the pressure drag coefficient assumes a substantially significant value in the range of 1.0 - 1.42. Such a high value of drag coefficient is particularly valid for bluff bodies with noncircular cross-sections with the sharp corners.

#### Keywords:

Bluff body; pressure drag; streamline  
body; fore body

Copyright © 2019 PENERBIT AKADEMIA BARU - All rights reserved

## 1. Introduction

The base flow field is a critical study to understand the practical problem which has various applications in the automobile industry. When the front body or the base has the blunt base will result in the wake formation resulting in sub-atmospheric pressure, and that results in colossal drag at critical Mach numbers. Any drag reduction will result in increasing the efficiency of the engine and savings in the energy, as fossil fuels are depleting in nature. Fossil fuels may be available only for the next twenty-five years. Hence, there is a need to design the aerodynamic shape in such a way that results in minimum drag. Most of the study conducted in the field of base flows were mostly experimental. In view of the cost involved in the wind tunnel test, simulation of such flows

\* Corresponding author.

E-mail address: [abdul.aabid@live.iium.edu.my](mailto:abdul.aabid@live.iium.edu.my) (Abdul Aabid)

numerically is need of the hour. From the numerical results, we can arrive at the optimum solution and hence, reduction in the number of wind tunnel runs.

Sowoud *et al.*, [1] investigated experimentally with the non-circular cylinder shape in order to visualize the flow field, estimate the pressure coefficient ( $C_p$ ), and the front body drag. In their study, they investigated the pressure coefficient at different velocities (that is 15.34 m/s, 20.38 m/s, and 26.84 m/s), the pressure coefficient ( $C_p$ ) is determined for with and without pipe. After the pressure coefficient,  $C_p$  has determined the drag coefficient,  $C_D$  for both cases with and without pipe cases. Since the simulation results were not available for this problem, hence the present study focuses attention on numerical simulation using Ansys software. Hence, their experimental results were validated with the simulation results.

Suresh *et al.*, [2] have found the drag coefficient through the simulations. They found the net drag coefficient ( $C_D$ ) and did not mention anything about the pressure coefficient, which is essential here to compare the results, especially for the base pressure and hence the base drag. The experimental results of Sowoud *et al.*, [1] are to validate their experimental results from the simulation results. Sajali *et al.*, [3] run the simulation test to discover the flow field and pressure coefficient,  $C_p$  of the non-circular cylinder shape. However, they studied only at the speed of 20.38m/s and their distance of a front body of a non-circular cylinder with 0 mm and 100 mm. The author labels the 0 mm and 100 mm distance of a front body of the non-circular cylinder as without pipe and with pipe respectively. Then, the flow field is shown in term of pressure, temperature, density, and Mach number. Thus, this study is a continuation of their work to show the influence of the distance of the front body of the non-circular cylinder and validate the pressure coefficient ( $C_p$ ) with the speed of 26.84 m/s.

Khan *et al.*, [4-8] obtained the effectiveness of microjets to control the based pressure by using a convergence-divergence nozzle with sudden expansion. The authors used the simulation results to compare with the experimental result with different parameter studies, which are the area ratio, length to diameter ratio, and NPR at different Mach number. Khan *et al.*, [9, 10] identified the supersonic flow over a delta wing through an ANSYS simulation. Used the microjets to study the flow development [11-15] and pulse jet for heat transfer augmentation by using ANSYS [16]. A dimensionless ratio of the pressure is known as the pressure coefficient ( $C_p$ ) is commonly used to compare different pressures around a bluff body for a variety of flow conditions. The pressure coefficient,  $C_p$  compares the pressure on the surface of the non-cylinder,  $P$ , to that at infinity,  $P_\infty$  [17]. An approximate formula was introduced by using a semi-empirical relation by Garabedian for the drag of an isolated disk with a cavity wake, where  $C_D$  is the drag coefficient of the drive based on its diameter [18].

The nature of the wake also affects the bluff body itself [19]. Next, the boundary layer affects the wake around the bluff body [20]. There are also three different types of flow regimes and pattern could be identified for strakes close to the corner, optimum strakes configuration, and the third strikes close to the center. There is another factor that contributes towards drag reduction is the suction over the windward face [21]. There are two forms of separations from bluff bodies; they are the sharp-edged, and the continuous surface where the boundary layer is unable to resist some critical adverse pressure gradient [22]. The measurements on circular cylinders have demonstrated that a curved or serrated separation line restrained the periodic vortex shedding. Therefore, producing a steady base flow behind the cylinder and a corresponding increase in the base pressure [23]. The Computational Fluid Dynamics (CFD) is a numerical technique used to solve equations regarding fluid flow and heat transfer problems inside a defined flow geometry [24, 25].

From the literature, most of the studies has been found for flow development using different object such as nozzle. Moreover, bluff body has been utilized for experimental study in order to

optimize the pressure and drag coefficient. However, theoretically it is intensely to obtain the visualization of the flow field by using the analytical approach. The visualization of the flow field from the experimental method is also a challenging task. This is because the visualization of the flow field needs to have a proper experimental setup and high cost of work. Therefore, the current focus of the study is to compute the flow field of a noncircular cylinder with the different distance of the front body and validate the pressure coefficient ( $C_p$ ) with the flow velocity 26.84 m/s. Thus, can get the simulation result and can compare to the experimental result with saving costs.

## 2. Methodology

In this study, the finite element analysis is used for solving the problem of fluid flow for a non-circular cylinder. ANSYS software is utilized as a technique of modeling and simulation of flow fields that provide accurate results [26].

### 2.1 Pressure Distribution

The geometry of the finite element for fluid flow based on the designed square plate front body on the drag reduction and pressure distribution of a bluff body is shown in Figure 1. The square plate front body of a bluff body is designed which is 108 mm of length, and 100 mm of the width of the rear body [1] is formed to investigate the flow structure on the blunt-edged body. Further, the term called Vortex Flow Experiment (VFE-2). The primary objective of the VFE-2 test was to validate the results of Navier-Stokes calculations and to obtain more detailed experimental data. The VFE-2 experiments were carried out for both sharp and blunt leading-edge shape delta wing [27-29].

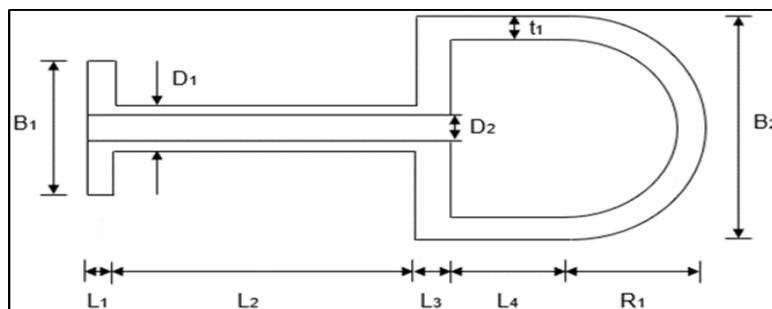


**Fig. 1.** The geometry of 2D square plate front body of a bluff body

The dimensions of the square plate bluff body are mentioned in Table 1.

**Table 1**

The dimension of 2D square plate front body of a bluff body

B1	B2	D1	D2	L1	L2	L3	L4	R1	t1
25 mm	100 mm	10 mm	8 mm	10 mm	0.25B2 to 1.75B2 mm	15 mm	43 mm	50 mm	8 mm

### 2.2 Two-Dimensional Finite Element Model and Meshing

The two-dimensional (2D) model of a bluff body with 0 mm distance of a square plate front body is shown in Figure 2(a). The two-dimensional (2D) model of a bluff body with a 100 mm distance of a square plate front body is shown in Figure 2(b). Both the 2D models were created by using ANSYS workbench [30].

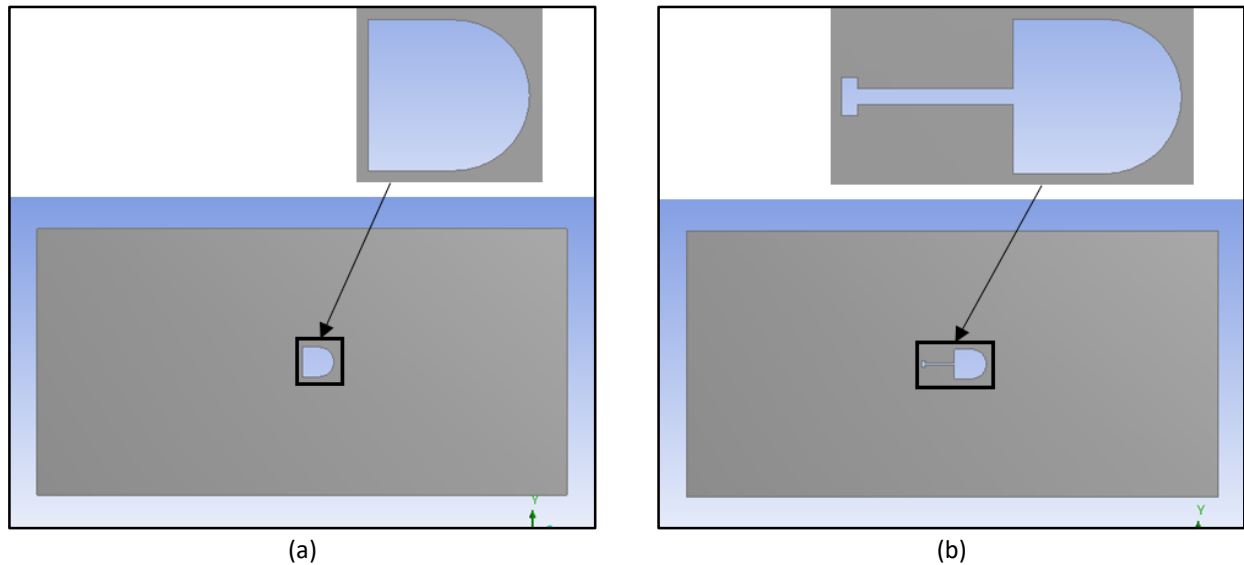


**Fig. 2.** 2D planar fluid body finite element (a) 0 mm and (b) 100 mm

The final form of finite element meshing for a 2D model of a bluff body with 0 mm distance of a square plate front body is shown in Figure 3(a). Total, 20320 binary nodes were generated for the 2D planar model. The final form of finite element meshing for a 2D model of a bluff body with a 100 mm distance of a square plate front body is shown in Figure 3(b). Total, 43140 binary nodes were generated for the 2D planar model. Both the 2D models were created by using ANSYS workbench for an unstructured mesh with the number of elements that have been used were high to enhance the mesh quality.

The meshing of the finite element for fluid flow and the number of elements used must be high to create a fine mesh in the close area at the edge of the planar body. It produces the most appropriate mesh for accurate and efficient solutions [31]. In the present case, the fine mesh is used with the number of divisions for edge sizing is 100 for all cases. The mesh is fine at the bluff body because we need to see the precise result for the bluff body. The volume area need not have high mesh. The triangle shape was used for an unstructured mesh with refinement to get smooth triangle shape of mesh with a high number of the element.

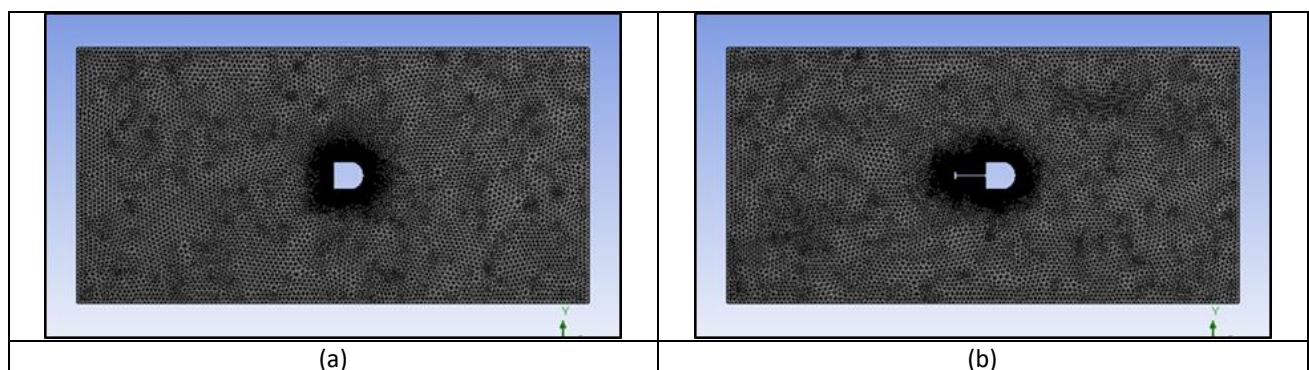


**Fig. 3.** 2D planar fluid body meshing (a) 0 mm and (b) 100 mm

### 2.3 Meshing Independence Study

The grid independence study has been done with three relevance center which is for coarse, medium and fine in order to see which test has the closest value with the experimental result for 0 mm distance of front body. The test results that the coarse test has some different value as compared

with the experimental results, while for medium and fine mesh have similar results when compared with the experimental result. Thus, the fine mesh has been selected for this study to evaluate the simulation result to compare with the experimental result. The meshing independence study is shown in Table 2.

**Table 2**

The meshing independence study for 0 mm distance of front body

Mesh Type	No. of Element	CFD Runtime	Total Pressure
Coarse	26840	192 seconds	-61.3961 Pa
Medium	30368	372 seconds	-55.7733 Pa
Fine	39464	691 seconds	-54.7262 Pa

### 2.4 Validation of Finite Element Results

In order to validate our present FE model, considered the experimental work of Sowoud *et al.*, [1]. Sowoud *et al.*, [1] have conducted experiments at the velocity of 15.34 m/s, 20.38 m/s and 26.84 m/s for without and with pipe to see the flow field, to investigate the pressure coefficient ( $C_p$ ) and to determine the drag coefficient ( $C_D$ ). By comparing the experimental results of Sowoud *et al.*, [1], and the present simulation result, the pressure coefficient,  $C_p$  is comparable where the difference between each method is minimal and are in an acceptable limit. However, the graph of pressure coefficient,  $C_p$  from the simulation is slightly different when compared with the experimental results of the pressure coefficient,  $C_p$ . The difference in the results may be due to the unstructured mesh.

The results of the pressure coefficient,  $C_p$  from simulation also is not smooth as compared to the experimental values as shown in Figure 4(a) and Figure 4(b). The results indicate that the simulation values show fluctuations as compared to the results from experiments. This is because the results obtained from the simulation have a large number of data points, whereas the experiments were performed for limited discrete points.

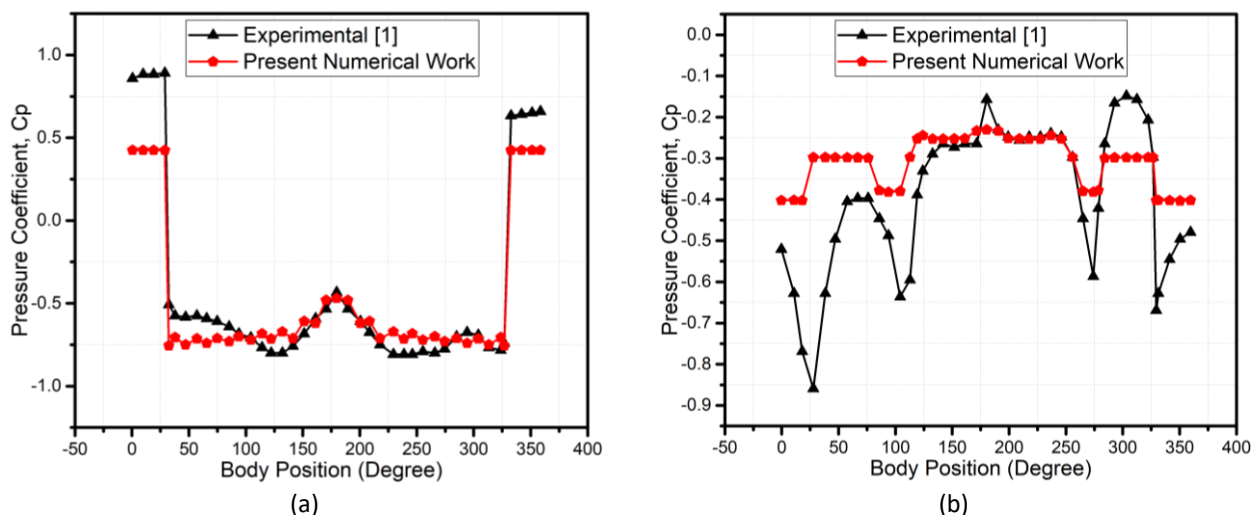


**Fig. 4.** Validation of result for 26.84 m/s (a) 0 mm and (b) 100 mm

### 3. Results

In this section, discussed the results of the simulations for different velocities and the distances between the front and rear body for the problem as shown in Figure 1. The ANSYS software already has the equations that required to proceed with calculation such as partial differential equation,

ordinary differential equation, and the energy equation. Hence, in this study used several equations and boundary condition to calculate the parameters.

### 3.1 Pressure Distribution

In this section the pressure variation from the inlet to the outlet of the 2D model of a bluff body for 0 mm, 25 mm, 50 mm, 75 mm, 100 mm, 125 mm, 150 mm and 175 mm distances of square plate front body with a velocity of 26.84 m/s. This pressure variation consists of total pressure only. A numerical study was performed to accomplish and verified each [32]. The Figure 5, 6, 7, 8, 9, 10, 11 and 12 show total pressure variation from the inlet to the outlet of the 2D model of a bluff body for 0 mm, 25 mm, 50 mm, 75 mm, 100 mm, 125 mm, 150 mm and 175 mm distances of square plate front body by considering contours (Figure 5(a), 6(a), 7(a), 8(a), 9(a), 10(a), 11(a) and 12(a)) and plots respectively (Figure 5(b), 6(b), 7(b), 8(b), 9(b), 10(b), 11(b) and 12(b)).

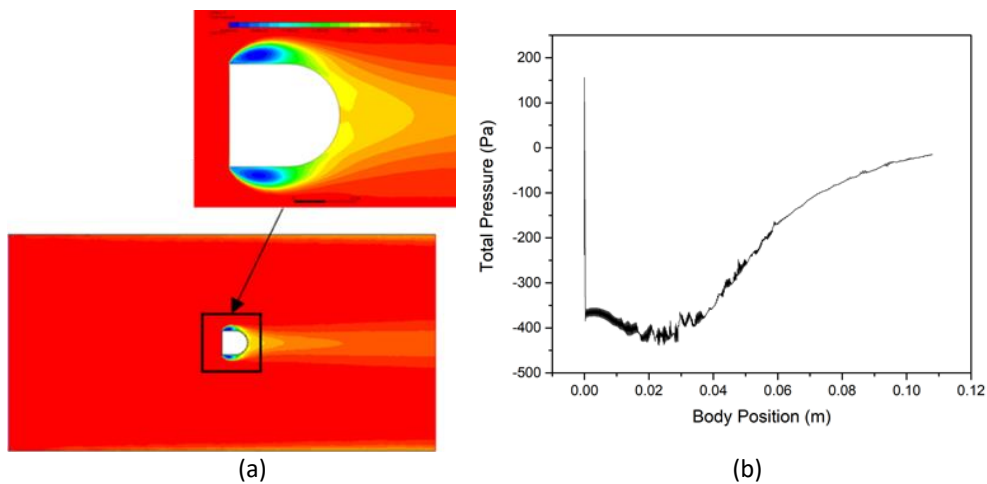


**Fig. 5.** Total pressure for 0 mm distance of front body (a) contours and (b) plot

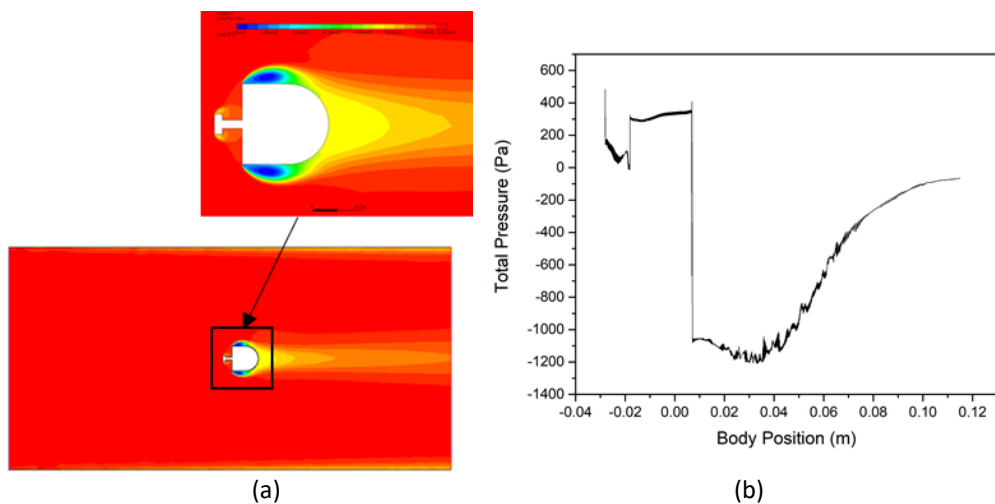


**Fig. 6.** Total pressure for 25 mm distance of front body (a) contours and (b) plot



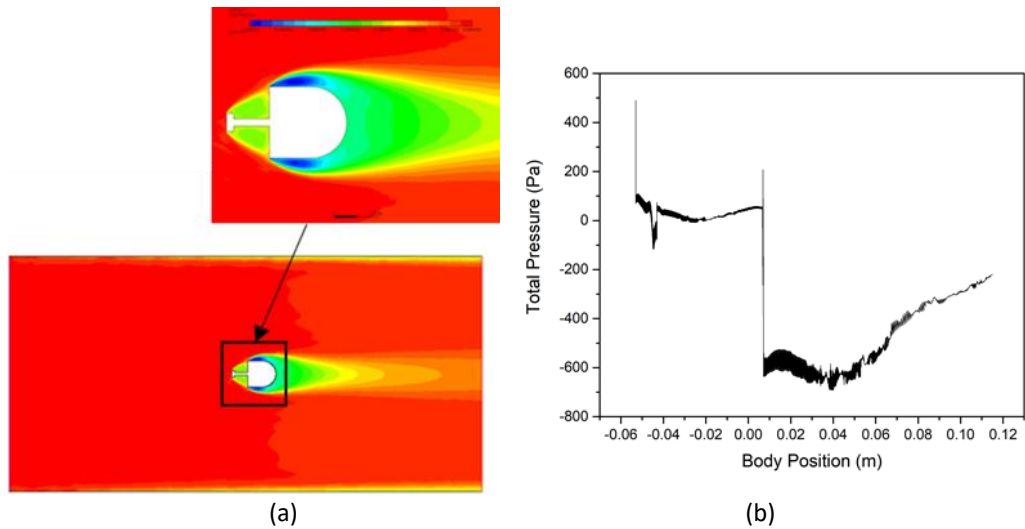


**Fig. 7.** Total pressure for 50 mm distance of front body (a) contours and (b) plot

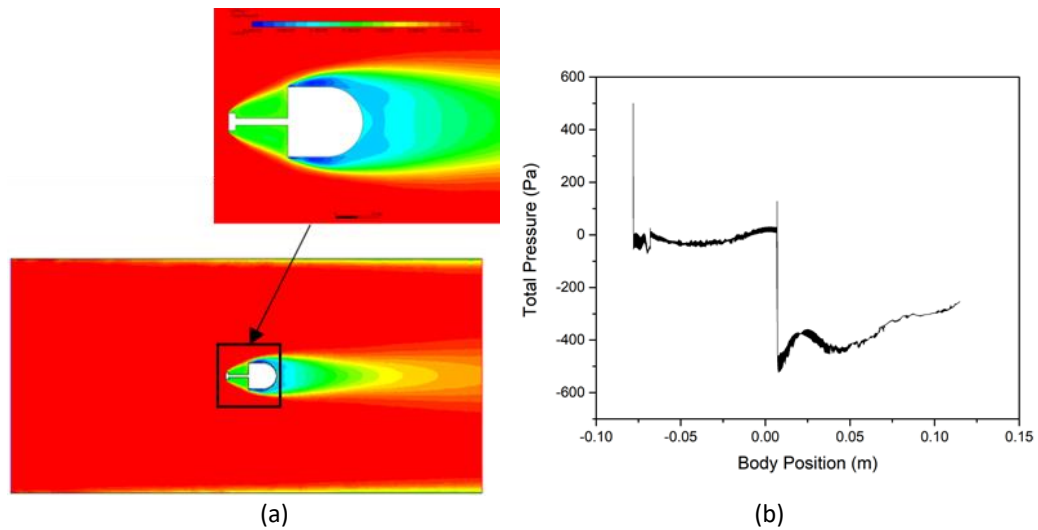


**Fig. 8.** Total pressure for 75 mm distance of front body (a) contours and (b) plot

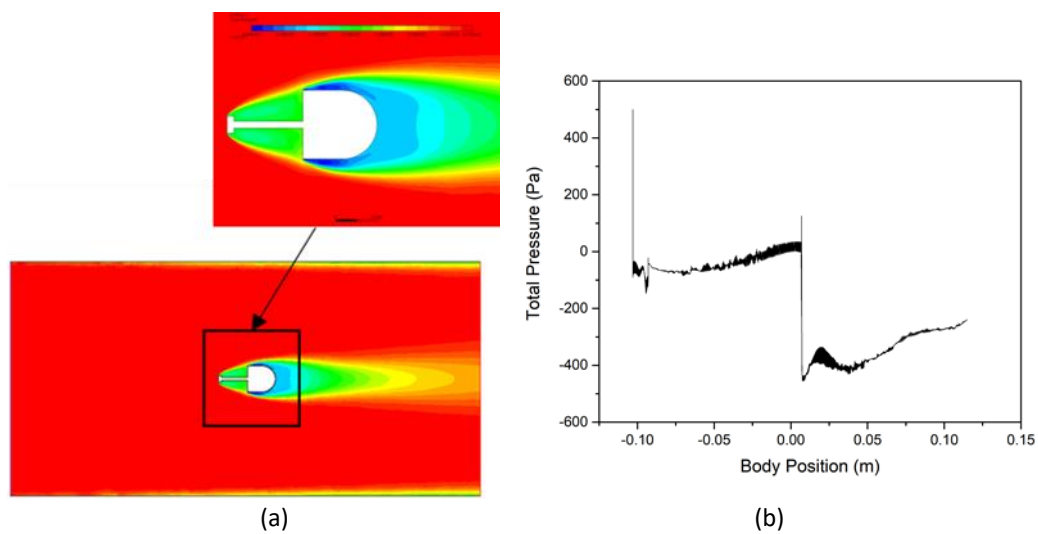


**Fig. 9.** Total pressure for 100 mm distance of front body (a) contours and (b) plot

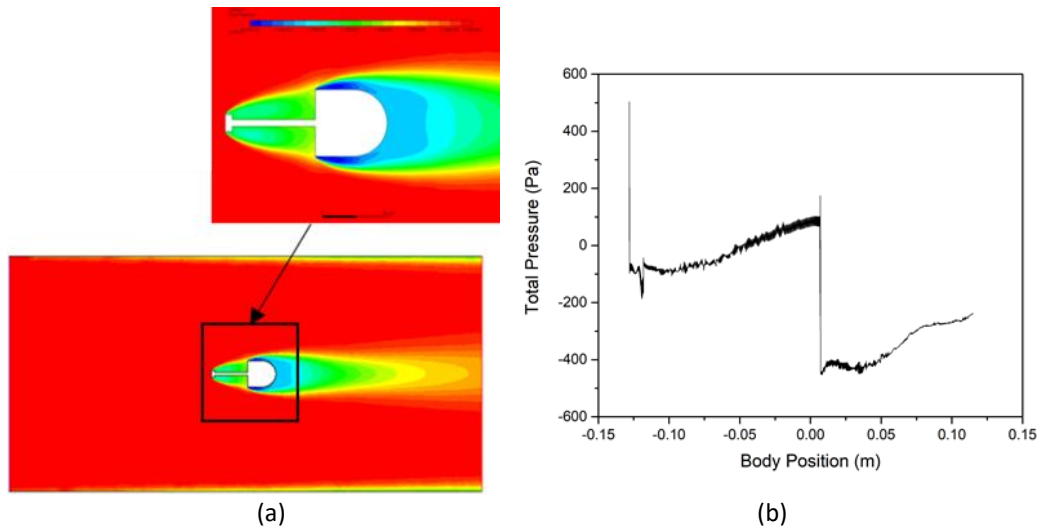


**Fig. 10.** Total pressure for 125 mm distance of front body (a) contours and (b) plot

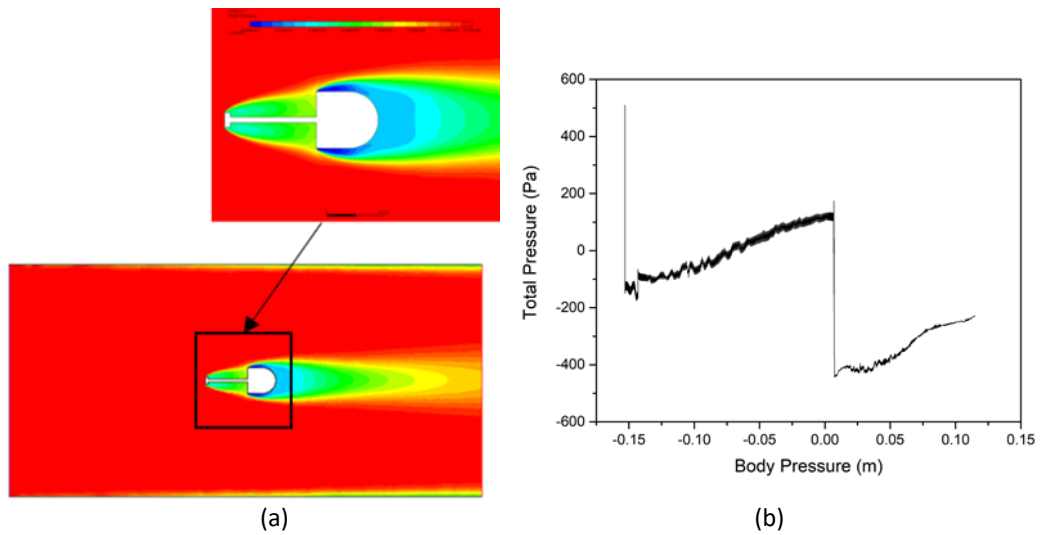


**Fig. 11.** Total pressure for 150 mm distance of front body (a) contours and (b) plot

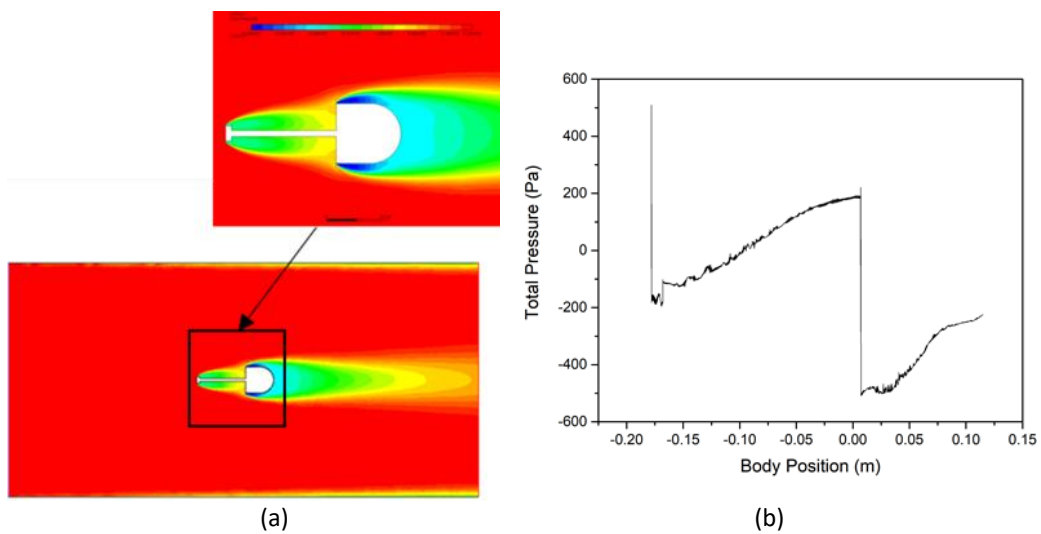


**Fig. 12.** Total pressure for 175 mm distance of front body (a) contours and (b) plot



### 3.2 Mach Number

In this section shows the velocity variation from the inlet to the outlet of the 2D model of a bluff body for 0 mm, 25 mm, 50 mm, 75 mm, 100 mm, 125 mm, 150 mm and 175 mm distances of square plate front body with a velocity of 26.84 m/s. This velocity variation consists of Mach number only. A numerical study was performed to obtain and verify each. The Figure 13, 14, 15, 16, 17, 18, 19 and 20 show Mach number variation from the inlet to the outlet of the 2D model of a bluff body for 0 mm, 25 mm, 50 mm, 75 mm, 100 mm, 125 mm, 150 mm and 175 mm distances of square plate front body by considering contours (Figure 13(a), 14(a), 15(a), 16(a), 17(a), 18(a), 19(a) and 20(a)) and plots respectively (Figure 13(b), 14(b), 15(b), 16(b), 17(b), 18(b), 19(b) and 20(b)).

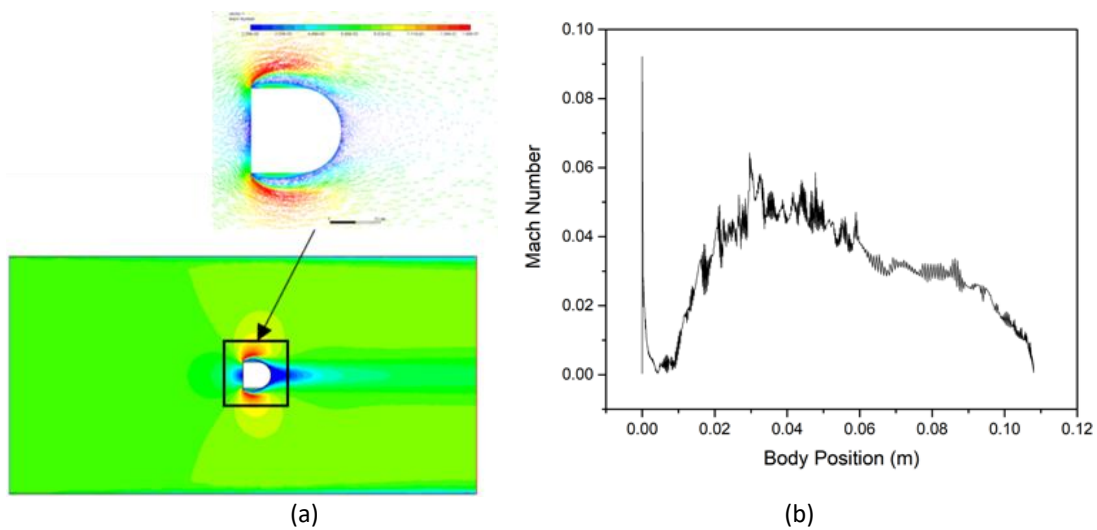


**Fig. 13.** Mach number for 0 mm distance of front body (a) contours and (b) plot

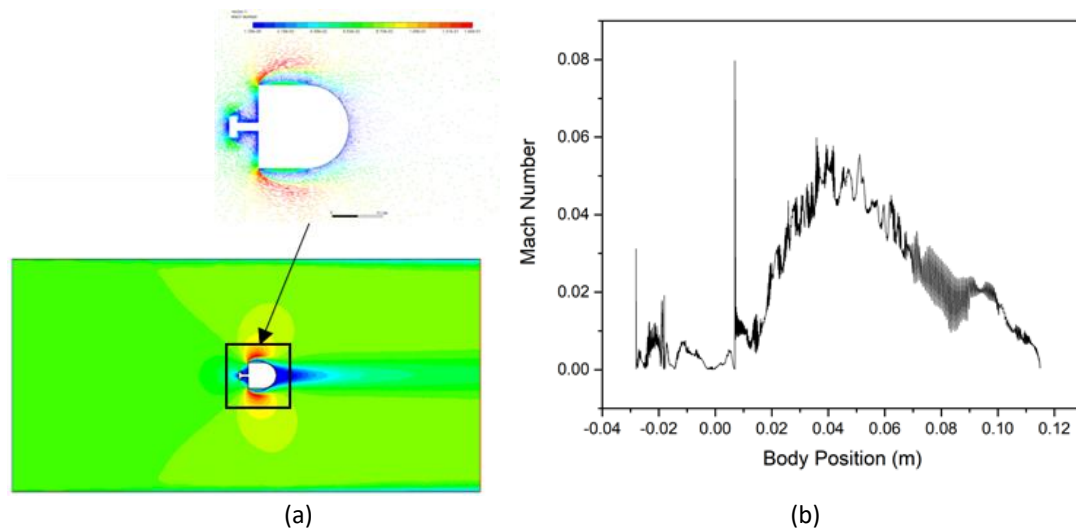


**Fig. 14.** Mach number for 25 mm distance of front body (a) contours and (b) plot

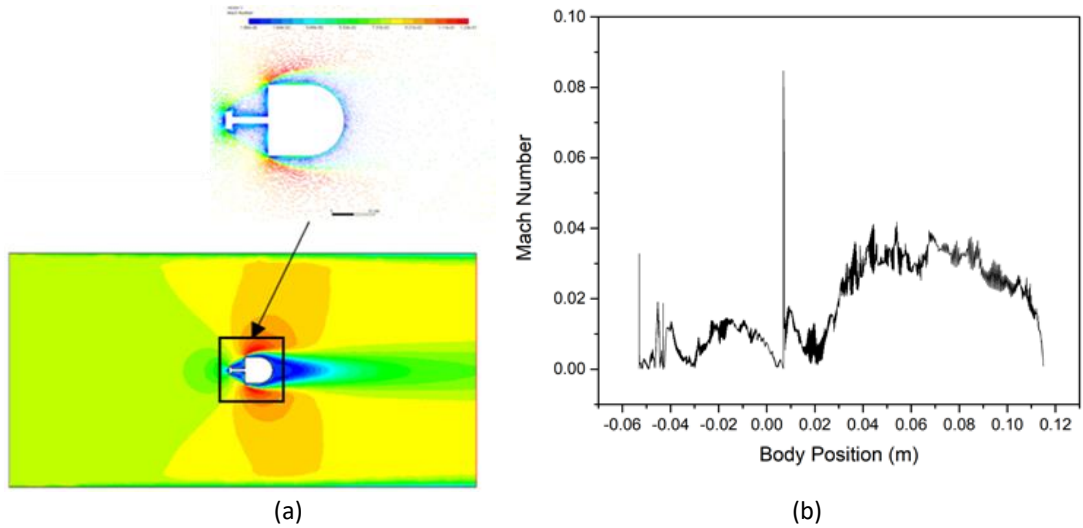


**Fig. 15.** Mach number for 50 mm distance of front body (a) contours and (b) plot

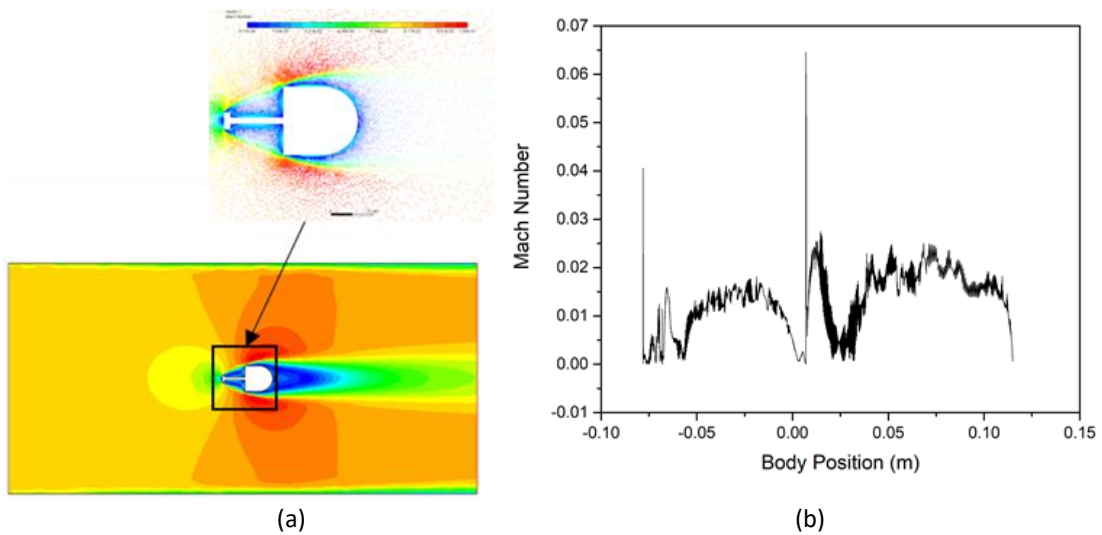


**Fig. 16.** Mach number for 75 mm distance of front body (a) contours and (b) plot

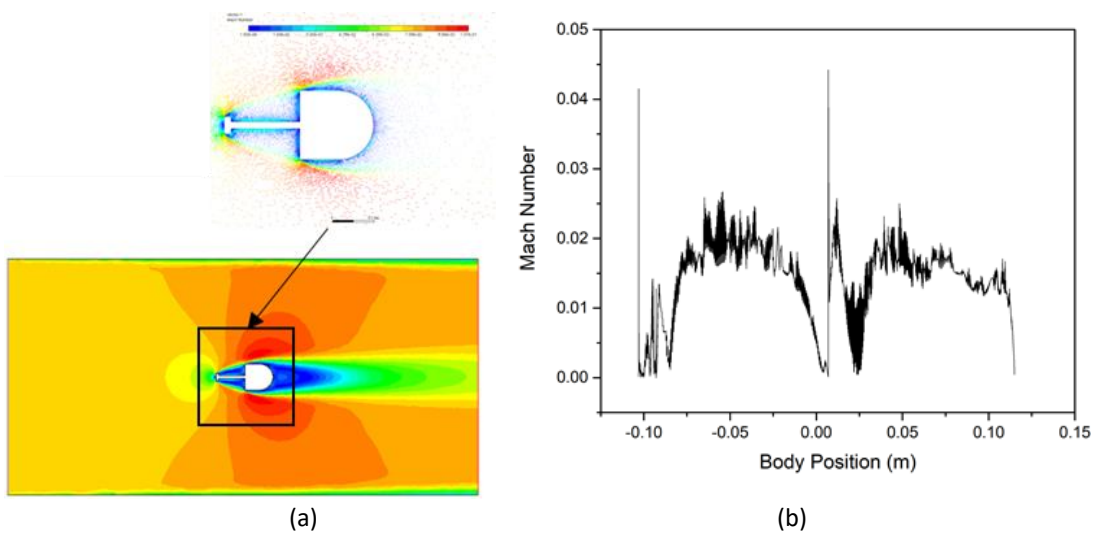


**Fig. 17.** Mach number for 100 mm distance of front body (a) contours and (b) plot

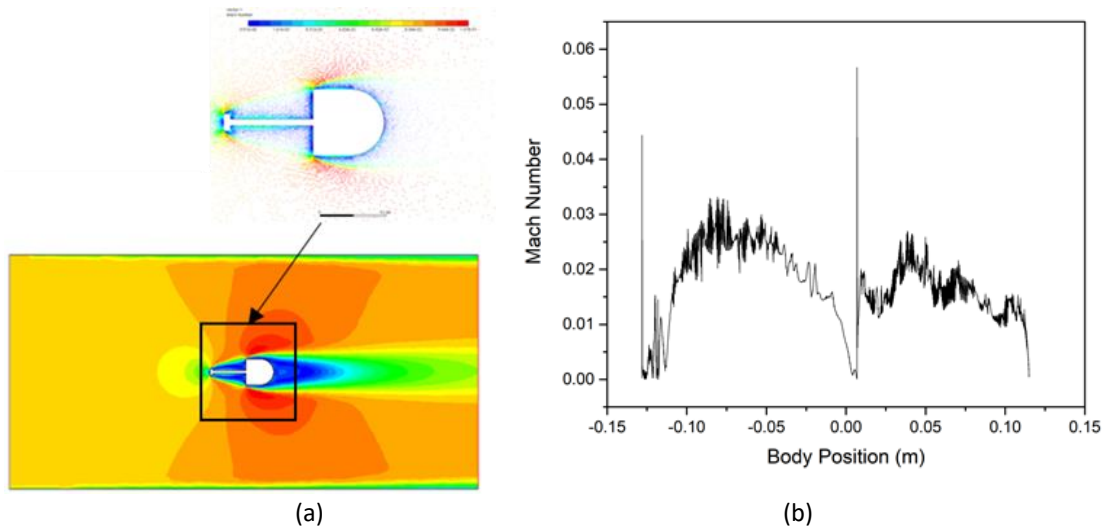


**Fig. 18.** Mach number for 125 mm distance of front body (a) contours and (b) plot

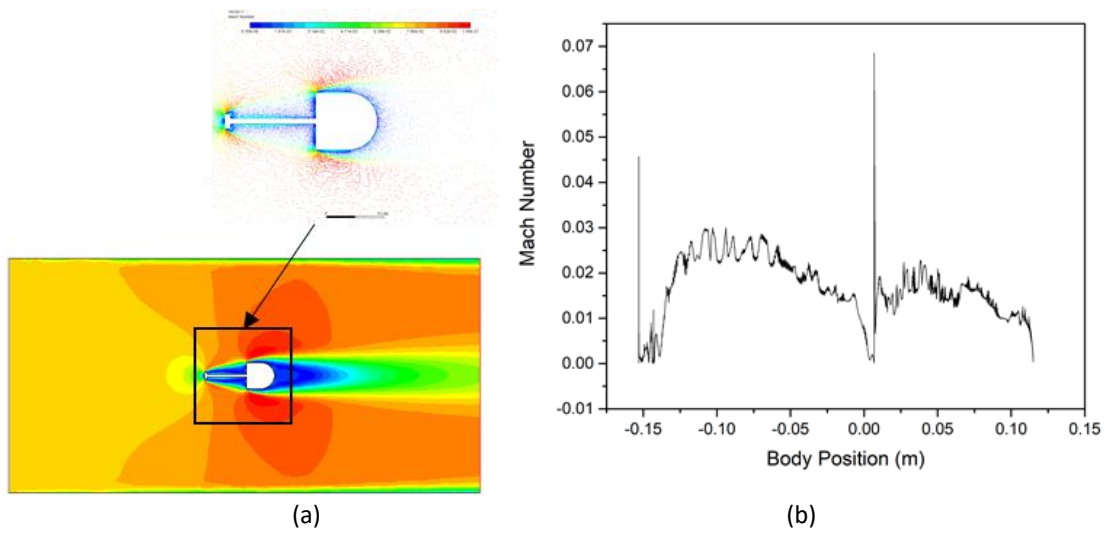


**Fig. 19.** Mach number for 150 mm distance of front body (a) contours and (b) plot

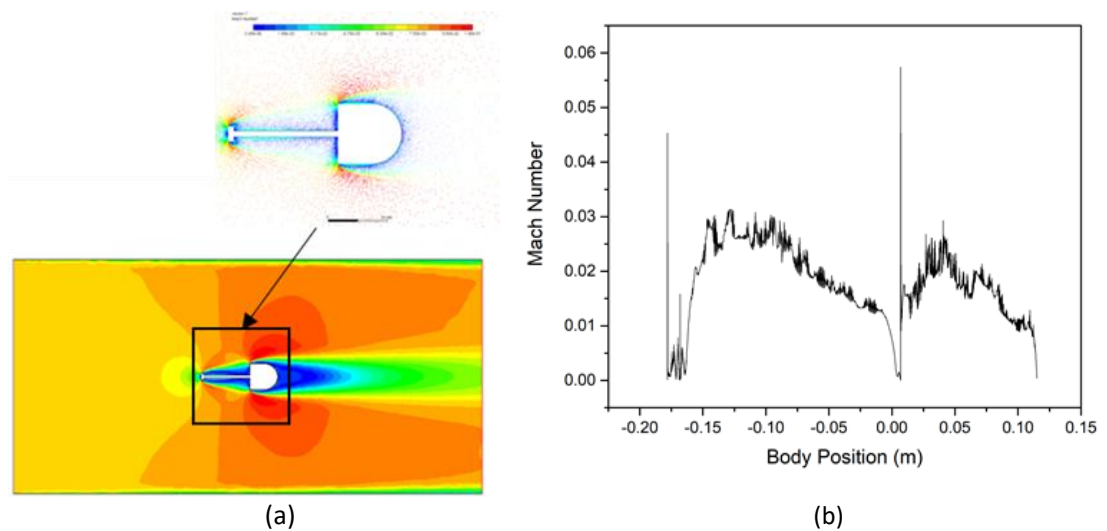


**Fig. 20.** Mach number for 175 mm distance of front body (a) contours and (b) plot

#### 4. Conclusions

The simulation of a non-circular cylinder with various distance of front body has been successfully studied by using an analytical and numerical method. The dimensionless terms for pressure coefficient are used and compared with the experimental result. The Bernoulli equation is also used as used by [1-3] for analytical calculation in ANSYS software. Furthermore, the ANSYS software is used to generate the non-circular cylinder flow field numerically and to prove the analytical method from research papers of [1-3]. From the simulation result, it is seen that a large wake zone at the back of the non-circular cylinder is formed. The flow field streamlines from the simulation result are smooth with the colors variation. The difference between all cases which are 0 mm, 25 mm, 50 mm, 75 mm, 100 mm, 125 mm, 150 mm, and 175 mm distances of square plate front body, it shows the different flow field for all cases. The results show that the flow field from the numerical method is the same as seen from the research papers from [1-3].

#### References

- [1] Sowoud, Khalid M., and E. Rathakrishnan. "Front body effects on drag and flow field of a three-dimensional noncircular Cylinder." *AIAA Journal* 31, no. 7 (1993): 1345-1347.
- [2] Suresh, V., P. S. Premkumar, and C. Senthilkumar. "Drag reduction of non-circular cylinder at subcritical Reynolds numbers." *Journal of Applied Fluid Mechanics* 12, no. 1 (2019): 187-194.
- [3] Muhammad Fahmi Mohd Sajali, Abdul Aabid, Sher Afghan Khan, Fharukh Ahmed Ghasi Mehaboobali, and Erwin Sulaeman. "Numerical investigation of flow field of a non-circular cylinder." *CFD Letters* 11, no. 5 (2019): 37-49.
- [4] Sher Afghan Khan, Abdul Aabid, Fharukh Ahmed Mehaboobali Ghasi, Abdulrahman Abdullah Al-Robaian, and Ali Sulaiman Alsagri. "Analysis of area ratio in a CD nozzle with suddenly expanded duct using CFD method." *CFD Letters* 11, no. 5 (2019): 61-71.
- [5] Fharukh, Ahmed GM, Abdulrehman A. Alrobaian, Abdul Aabid, and Sher Afghan Khan. "Numerical analysis of convergent-divergent nozzle using finite element method." *International Journal of Mechanical and Production Engineering Research and Development* 8, no. 6 (2018): 373-382.
- [6] Khan, Sher Afghan, Abdul Aabid, and Maughal Ahmed Ali Baig. "CFD analysis of CD nozzle and effect of nozzle pressure ratio on pressure and velocity for suddenly expanded flows." *International Journal of Mechanical and Production Engineering Research and Development* 8 (2018): 1147-1158.
- [7] Khan, Ambareen, Abdul Aabid, and Sher Afghan Khan. "CFD analysis of convergentdivergent nozzle flow and base pressure control using micro-JETS." *International Journal of Engineering and Technology* 7, no. 3.29 (2018): 232-235.
- [8] Pathan, Khizar Ahmed, Prakash S. Dabeer, and Sher Afghan Khan. "Optimization of area ratio and thrust in suddenly expanded flow at supersonic Mach numbers." *Case studies in thermal engineering* 12 (2018): 696-700.
- [9] Khan, Sher Afghan, Abdul Aabid, and C. Ahamed Saleel. "CFD simulation with analytical and theoretical validation of different flow parameters for the wedge at supersonic Mach number." *International Journal of Mechanical and Mechatronics Engineering* 1 (2019).
- [10] Sher Afghan Khan, Abdul Aabid, Imran Mokashi, Abdulrahman Abdullah Al-Robaian, and Ali Sulaiman Alsagri. "Optimization of two-dimensional wedge flow field at supersonic Mach number." *CFD Letters* 11, no. 5 (2019): 80-97.
- [11] Khan, Sher Afghan, Abdul Aabid, and C. Ahamed Saleel. "Influence of micro jets on the flow development in the enlarged duct at supersonic Mach number." *International Journal of Mechanical and Mechatronics Engineering* 19 (2019): 70-82.
- [12] Khan, S. A., Imran Mokashi, Abdul Aabid, and Mohammed Faheem. "Experimental research on wall pressure distribution in CD nozzle at Mach number 1.1 for area ratio 3.24." *International Journal of Recent Technology and Engineering* 8, no. 2S3 (2019): 971-975.
- [13] Azami, Muhammed Hanafi, Mohammed Faheem, Abdul Aabid, Imran Mokashi, and S. A. Khan. "Experimental research of wall pressure distribution and effect of micro jet at Mach." *International Journal of Recent Technology and Engineering* 8, no. 2S3 (2019): 1000-1003.
- [14] Azami, Muhammed Hanafi, Mohammed Faheem, Abdul Aabid, Imran Mokashi, and S. A. Khan. "Inspection of Supersonic Flows in a CD Nozzle using Experimental Method." *Int. J. Recent Technol. Eng* 8, no. 2S3 (2019): 996-999.

- [15] Khan, S. A., Abdul Aabid, and Zakir Ilahi Chaudhary. "Influence of control mechanism on the flow field of duct at Mach 1.2 for Area Ratio 2.56." *International Journal of Innovative Technology and Exploring Engineering* 8, no. 6S4 (2019): 1135–1138.
- [16] Umair, Siddique Mohd, Sher Afghan Khan, Abdulrahman Alrobaian, and Emaad Ansari. "Numerical study of heat transfer augmentation using pulse jet impinging on pin fin heat sink." *CFD Letters* 11, no.3 (2018): 84-91.
- [17] Libii, Josué Njock. "Using wind tunnel tests to study pressure distributions around a bluff body: the case of a circular cylinder." *World Transactions on Engineering and Technology Education* 8, no. 3 (2010): 361-366.
- [18] Koenig, Keith, and Anatol Roshko. "An experimental study of geometrical effects on the drag and flow field of two bluff bodies separated by a gap." *Journal of Fluid Mechanics* 156 (1985): 167-204.
- [19] Castro, I. P., and A. G. Robins. "The flow around a surface-mounted cube in uniform and turbulent streams." *Journal of Fluid Mechanics* 79, no. 2 (1977): 307-335.
- [20] Gowda, B. H. L., H. J. Gerhardt, and C. Kramer. "Surface flow field around three-dimensional bluff bodies." *Journal of Wind Engineering and Industrial Aerodynamics* 11, no. 1-3 (1983): 405-420.
- [21] Pamadi, B. N., C. Pereira, and B. H. Laxmana Gowda. "Drag reduction by strakes of noncircular cylinders." *AIAA Journal* 26, no. 3 (1988): 292-299.
- [22] Bearman, P. W. "Bluff body flows applicable to vehicle aerodynamics." *Journal of Fluids Engineering* 102, no. 3 (1980): 265-274.
- [23] Tanner, M. "Reduction of base drag." *Progress in Aerospace Sciences* 16, no. 4 (1975): 369-384.
- [24] Lomax, H, Pulliam, T.H., Zingg, D.W., and Kowalewski, T.A. 2002. "Fundamentals of computational fluid dynamics." *Applied Mechanics Reviews* 55 (4): B61.
- [25] Naga Sudhakar, B. V. V., B. Purna Chandra Sekhar, P Narendra Mohan, and Md Touseef Ahmad. "Modeling and simulation of convergent-divergent nozzle using computational fluid dynamics." *International Research Journal of Engineering and Technology (IRJET)* 3, no. 8 (2016): 346–350.
- [26] Stefanou, George. "The stochastic finite element method: past, present and future." *Computer Methods in Applied Mechanics and Engineering* 198, no. 9–12 (2009): 1031–1051.
- [27] Sher Afghan Khan, Abdulrahman Abdulla Al Robaian, Mohammed Asadullah, and Abdul Mohsin Khan. "Grooved cavity as a passive controller behind backward facing step." *Journal of Advanced Research in Fluid Mechanics and Thermal Sciences* 53, no. 2 (2019): 185–193.
- [28] Sher Afghan Khan, Abdulrahman A. Alrobaian, Mohammed Asadullah, and Aswin. "Threaded spikes for bluff body base flow control." *Journal of Advanced Research in Fluid Mechanics and Thermal Sciences* 53, no. 2 (2019): 194-203.
- [29] Hamizi, Ilya Bashiera, and Sher Afghan Khan. "Aerodynamics investigation of delta wing at low Reynold's number." *CFD Letters* 11, no. 2 (2019): 32-41.
- [30] Pathan, Khizar Ahmed, Sher Afghan Khan, and P. S. Dabeer. "CFD analysis of effect of area ratio on suddenly expanded flows." In *2017 2nd International Conference for Convergence in Technology (I2CT)*, pp. 1192-1198. IEEE, 2017.
- [31] Aabid, Abdul, Ambreen Khan, Nurul Musfirah Mazlan, Mohd Azmi Ismail, Mohammad Nishat Akhtar, and S A Khan. "Numerical simulation of suddenly expanded flow at Mach 2.2." *International Journal of Engineering and Advanced Technology* 8, no. 3 (2019): 457–462.
- [32] Pathan, Khizar Ahmed, Sher Afghan Khan, and P. S. Dabeer. "CFD analysis of effect of Mach number, area ratio and nozzle pressure ratio on velocity for suddenly expanded flows." In *2017 2nd International Conference for Convergence in Technology (I2CT)*, pp. 1104-1110. IEEE, 2017.